Available online at www.sciencedirect.com
SCIENCE DIRECT
Journal of Chromatography B, 837 (2006) 35–43
JOURNAL OF CHROMATOGRAPHY B
www.elsevier.com/locate/chromb

Characterization of the stability of a fully human monoclonal IgG after prolonged incubation at elevated temperature

Hongcheng Liu *, Georgeen Gaza-Bulseco, Joanne Sun

Protein Analytics, Process Sciences Department, 100 research Drive, Abbott Bioresearch Center, Worcester, MA 01605, USA

Received 13 December 2005; accepted 27 March 2006
Available online 27 April 2006

Abstract

The susceptible degradation sites of therapeutic proteins are routinely assessed under accelerated conditions such as exposure to chemicals or incubation at elevated temperature or a combination of both. A fully human monoclonal IgG_1 antibody was characterized after incubation at 40 °C for 6 months by employing mass spectrometry and chromatography analyses. It was found that deamidation, fragmentation and N-terminal glutamate cyclization to form pyroglutamate are the major degradation pathways. Three major deamidation sites were identified and one site in a small tryptic peptide accounted for more than 80% of the total. Peptide cleavage was observed at several positions between different pairs of amino acids. Most of the cleavage sites were located in the hinge or other flexible regions of the IgG molecule.

Keywords: Recombinant monoclonal antibody; Peptide mapping; Deamidation; Pyroglutamate

1. Introduction

Stability of monoclonal antibody therapeutics is an important aspect of characterization programs. The most reliable information can only be obtained by long-term monitoring of the stability at the normal storage conditions throughout the shelf-life of the products. However, in order to obtain information of the most susceptible degradation pathways and the most vulnerable sites of the molecules, stability of molecules can be assessed under extreme conditions such as elevated temperatures, exposure to chemicals, light, or a combination of the above. Whether or not the short-term accelerated stability information is predictive of long-term stability under normal storage conditions, valuable information on the nature of degradation pathways can be obtained within a short period of time.

In the study of the stability of a mouse IgG_1 and a IgG_{2a} monoclonal antibodies at different pHs and temperatures, Jiskoot et al. [1] reported that antibodies are more susceptible to degradation at 37 °C than at 4 °C. Irreversible aggregation was the major degradation pathway at low pH ranges, while peptide bond cleavage around the hinge region was the major degradation pathway at higher pH ranges. An acidic shift of the isoelectric focusing (IEF) profiles of the two antibodies at higher pH was also noticed, which the authors suggested could be caused by deamidation. Kroon et al. [2,3] reported the stability results of a mouse monoclonal IgG_{2a} antibody, OKT3. Peptide cleavage at the hinge region and the Fc constant region was observed after long-term storage at 5 °C, which is the normal storage condition for OKT3. Acidic shift of OKT3 was observed by both IEF and cation exchange chromatography after incubation at 37 °C for 2–6 weeks. Deamidation of asparagine (Asn) residues in the constant regions was the major degradation pathway at 37 °C, while at 2–8 °C, after long-term storage (>14 months), an additional deamidation site was found. Methionine oxidation at one site in the variable region and four sites in the constant region, oxidation of a tryptophan (Trp) in the variable region, and oxidation of a non-disulfide linked cysteine (Cys) residue in the complementarity determining region (CDR) were also observed after storage at 2–8 °C. Paborji et al. [4] studied the stability of a chimeric mouse–human monoclonal antibody. They found that when samples were incubated at 60 °C at higher pH, fragmentation was the major degradation pathway, while at lower pH range, aggregation was the major degradation pathway. In addition to fragmentation, degradation at high pH range also occurred through deamidation and disulfide bond breakage. Alexander and Hughes [5] also studied the

* Corresponding author. Tel.: +1 508 849 2591; fax: +1 508 793 488.
E-mail address: hongcheng.liu@abbott.com (H. Liu).

1570-0232/$ – see front matter © 2006 Elsevier B.V. All rights reserved.
doi:10.1016/j.jchromb.2006.03.053

thermal stability of a chimeric (human/mouse) monoclonal antibody at 60 °C for various lengths of time. Breakage of disulfide bonds and peptide cleavage at the hinge region were noticed. By noticing that the same degradation species were present at different time points, the authors concluded that cleavage by thermal stress was site-specific. Cordoba et al. [6] characterized non-enzymatic fragmentation of four humanized IgG_1 monoclonal antibodies under different temperatures (−20, 5, 30 or 40 °C) at pH 5.2. Two major cleavage sites were identified to locate in the same hinge region sequence of the four different IgG_1 antibodies and these cleavage sites were not affected by protease inhibitors or host cell proteins. An acidic shift, presumably due to deamidation, was also reported for a humanized IgG monoclonal antibody, h1B4 [7] and a mouse monoclonal antibody, MMA383 [8] after incubation at conditions favoring deamidation.

In this study, a fully human monoclonal IgG_1 antibody after storage at 40 °C for 6 months at pH 5.2 was analyzed side-by-side with the same antibody stored at −80 °C by multiple analytical techniques. Multiple peptide bond cleavage sites were identified by mass spectrometry following either size exclusion or reverse-phase chromatography. Three Asn deamidation sites and one glutamine (Gln) deamidation site were identified by peptide mapping and mass spectrometry. The original N-terminal glutamate (Glu) was found to partially degrade to pyroglutamate by matrix-assisted-laser-desorption-ionization time-of-flight (MALDI-TOF) mass spectrometer and enzymatic digestion.

2. Experimental

The fully human monoclonal IgG_1 antibody was produced by a transfected Chinese hamster ovary cell line (CHO) and purified by several chromatography steps including cation exchange, anion exchange and hydrophobic interaction chromatography. Sample at 50 mg/mL in formulation buffer (5.57 mM sodium phosphate monobasic, 8.69 mM sodium phosphate dibasic, 106.69 mM sodium chloride, 1.07 mM sodium citrate, 6.45 mM citric acid, 66.68 mM mannitol and 0.1% Tween) at pH 5.2 was incubated at 40 °C for 6 months. The same antibody at approximately 70 mg/mL in the same buffer stored at −80 °C was used as a control.

A Shimadzu HPLC (Shimadzu) and a Superose-6 column (Amershan Bioscience of GE healthcare) were used for size exclusion chromatography (SEC) analysis. Forty micrograms of each sample were loaded and then eluted isocratically using an eluent of 20 mM sodium phosphate (J.T. Baker), 150 mM sodium chloride (J.T. Baker), pH 7.5 at a flow-rate of 0.5 mL/min. Elution was monitored at UV 214 and 280 nm. Peaks were collected and concentrated using centrifugal filter devices with a 5 kDa MW cut-off (Millipore). The concentrated fractions were analyzed using Q Star pulsar i LC–MS/MS mass spectrometer (Applied Biosystems).

A Shimadzu HPLC and a C4 reverse-phase column (Vydac, 250 mm × 4.6 mm i.d., 5 μm particle size, 300 A pore size) were used for analysis of intact antibody and antibody after reduction. To reduce the antibody, samples were diluted to a final concentration of 10 mg/mL with phosphate buffered saline (PBS) and then incubated with dithiothreitol (DTT) (Sigma) at a final concentration of 10 mM at 37 °C for 30 min. Samples were loaded at 95% eluent A (0.02% trifluoroacetic acid (TFA) (J.T. Baker), 0.08% formic acid (FA) (Sigma) in Milli-Q water) and 5% eluent B (0.02% TFA, 0.08% FA in acetonitrile (EMD)), and then eluted by increasing the percentage of eluent B. Separation of fragments from intact antibody and from free light chain and heavy chain after reduction was optimized. The column oven temperature was set at 60 °C. All individual peaks were collected and concentrated using a speed-vacuum and analyzed using mass spectrometry.

For peptide mapping, samples were denatured with a final concentration of 6 M guanidine hydrochloride (J.T. Baker) in 10 mM ammonium bicarbonate (Sigma) at room temperature for 15 min. Samples were then reduced by incubating with 10 mM DTT at 37 °C for 60 min. The reduced samples were alkylated by iodoacetic acid (Sigma) at a final concentration of 50 mM after adjusting the pH to approximately 7.0 with 1 M Tris, pH 8.0, at 37 °C for 30 min. Samples were then dialyzed against 10 mM ammonium bicarbonate at 4 °C overnight using Spectra/Por 6–8000 MW cut-off membrane tubing (Spectrum Laboratories Inc.). Samples were recovered and digested with trypsin (Promega) at a 1:20 (w/w) trypsin:IgG ratio at 37 °C for 4 h. Sample preparation for Lys-C digestion was the same as for trypsin as mentioned above. Samples were then analyzed using a Shimadzu HPLC and a C18 reverse-phase column (Vydac, 250 mm × 4.6 mm i.d., 5 μm particle size, 120 A pore size) using the same eluents as used for intact and reduced IgG analysis. Samples were loaded at 2% eluent B and then eluted by increasing eluent B from 2 to 35% in 140 min. The flow-rate was set at 1 mL/min and the column oven temperature was set at 60 °C. Elution was monitored at both 214 and 280 nm. For further analysis, peaks present only in the stability samples were collected and concentrated using a speed-vacuum. The concentrated fractions were analyzed using mass spectrometry.

A Q Star pulsar i LC–MS/MS system coupled with an Agilent HPLC (Agilent) system was used for intact molecular weight measurements of fractions collected from SEC and reverse-phase chromatography. Q Star was also used for MS/MS analysis of peptides to determine the sites of modifications. The eluents used were the same as described previously for intact, reduced IgG and for peptide mapping, but only a short gradient of increasing eluent B was used to elute the materials off the columns. For intact IgG, light chain, heavy chain and fragments, a C4 column was used (Vydac, 150 mm × 1 mm i.d., 5 μm particle size, 300 A pore size). For peptide MS/MS analysis, a C18 column (Vydac, 150 mm × 1 mm i.d., 5 μm particle size, 300 A pore size) was used and the collision energy was optimized for each individual peptide.

LCQ_{DECA}XP mass spectrometer (ThermoFinnigan) was used for the analysis of early eluting small peptides on C18 reverse-phase chromatography. Peptides were loaded onto a C18 column (Vydac, 150 mm × 1 mm i.d., 5 μm particle size, 300 A pore size) and then eluted using the reverse-phase eluents with a similar gradient for peptide mapping. To increase sensitivity, LCQ mass spectrometer was operated in the zoom scan mode only in

a narrow *m/z* range around 447 Da, which was the range for the peptide of interest.

An AXIMA-CFR plus X MALDI-TOF mass spectrometer (Shimadzu) was used for MALDI-TOF mass spectrometer analysis of peptides. The matrix was prepared by dissolving 10 mg of α-cyano-4-hydroxy-cinnamic acid (Sigma) in a final 50% acetonitrile, 1% TFA. Approximately 1 μL of sample was spotted on a MALDI plate first. After samples were air-dried, angiotensin (MH^+ of 1046.5 Da) and a synthesized peptide P14P (MH^+ of 1533.9 Da) (Both from Sigma) were overlaid on the same spots as internal standards. Finally, 1 μL matrix was applied on the spots. Data was acquired in the positive mode using reflectron. To remove pyroglutamate, one vial of pyroglutamate aminopeptidase (Sigma) was reconstituted in 50 μL of 10 mM ammonium bicarbonate buffer with 10 mM DTT and 1 mM EDTA, and then 1 μL of the reconstituted pyroglutamate aminopeptidase was added to the dried peptide fractions collected from 100 μg digested antibody after reconstitution in 10 μL of 10 mM ammonium bicarbonate. Digestion was carried out at 75 °C for 15 min.

3. Results

3.1. Aggregation and fragmentation

Samples were evaluated by SEC to detect fragments and aggregates. In both control and stability samples, less than 1% aggregate was observed. The control also had less than 1% fragments, while, the stability sample had 7.2% fragments (Fig. 1). In order to detect fragments that were still held together by non-covalent interactions, samples were also analyzed by reverse-phase chromatography before and after reduction (Figs. 2 and 3). Fragments collected from SEC as well as peaks labeled in Figs. 2 and 3 were analyzed by Q Star mass spectrometer. Identification of the peaks is summarized in Tables 1–3.

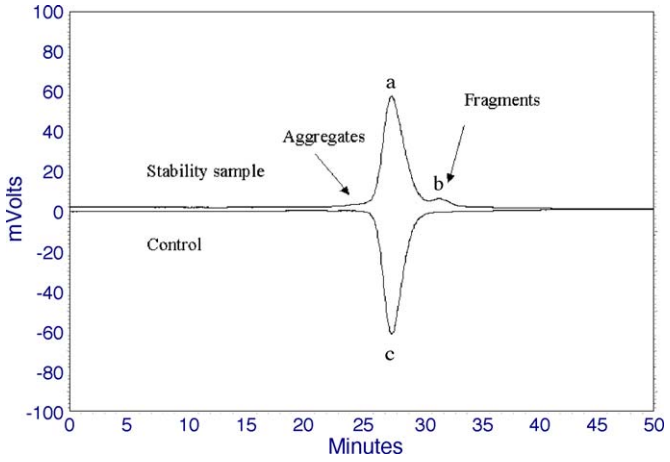

Fig. 1. SEC chromatograms of accelerated stability sample (40 °C for 6 months) and control (−80 °C) using a superpose-6 column and monitored by UV 280 nm. Peak b was collected, analyzed by mass spectrometry and summarized in Table 1.

3.2. Peptide mapping

A mirror image of peptides from the stability sample and control are shown in Fig. 4. Peptide patterns of the control and stability samples are similar except for the presence of four additional peaks (peaks 1–4 in Fig. 4) in the stability sample. These extra peaks from the stability samples were separately collected and analyzed by MALDI-TOF. Peaks 1, 2 and 4 had molecular weights of 1 Da higher than predicted from their amino acid sequences. All of the peptides contain either Asn or Gln residues, therefore the 1 Da difference could be a result of deamidation.

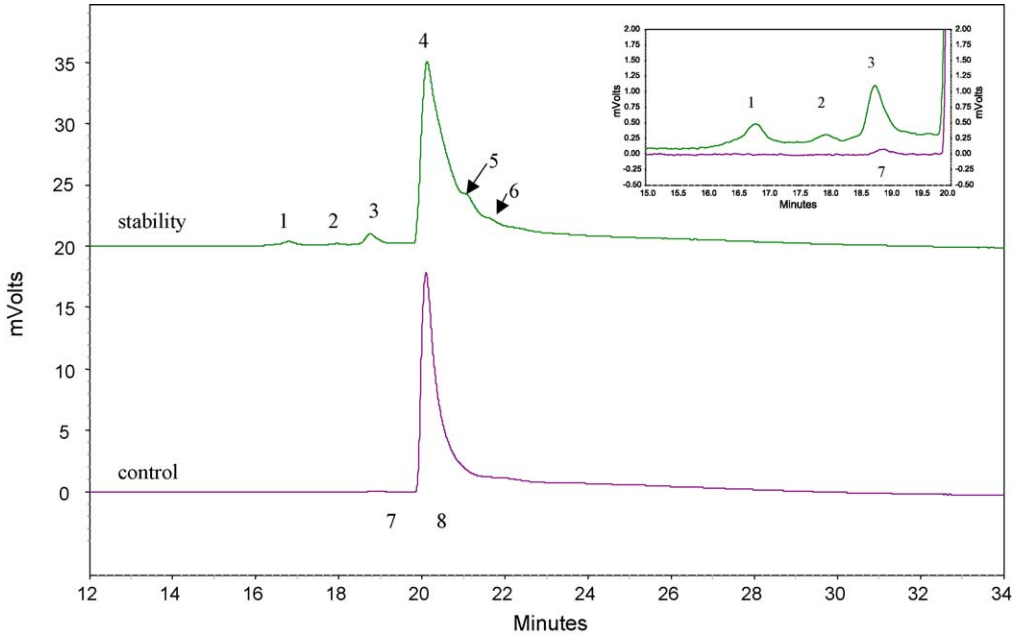

Fig. 2. Reverse-phase chromatograms of accelerated stability sample (40 °C for 6 months) and control (−80 °C) using a 250 mm × 4.6 mm Vydac C4 column and monitored using UV 280 nm. Portion of the chromatograms is enlarged as shown as inset. All labeled peaks were collected, analyzed by mass spectrometry and summarized in Table 2.

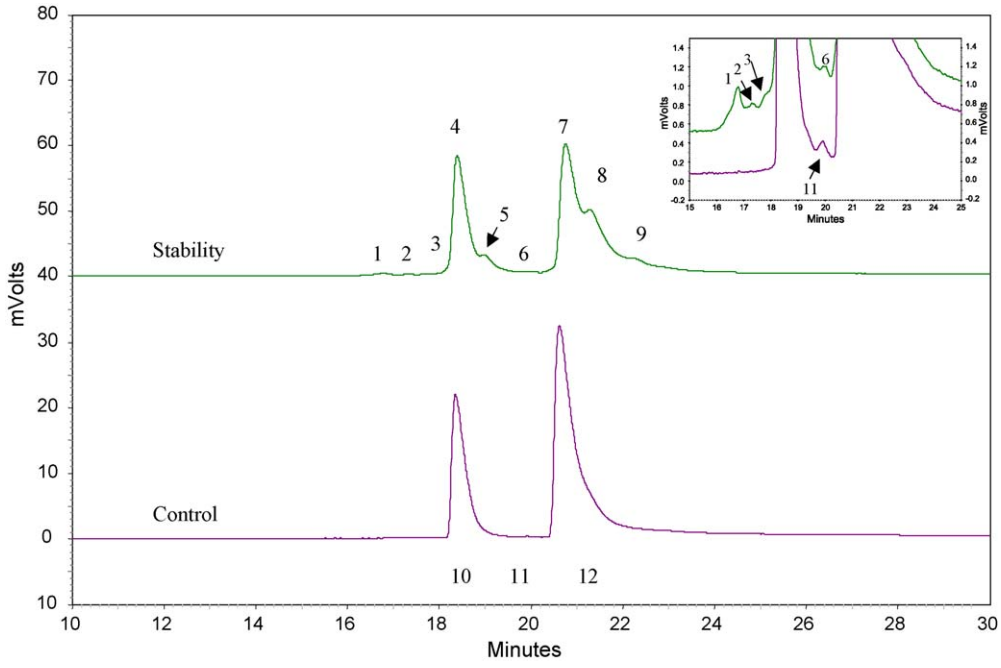

Fig. 3. Reverse-phase chromatograms of accelerated stability sample (40 °C for 6 months) and control (−80 °C) after reduction using a 250 mm × 4.6 mm Vydac C4 column and monitored using UV 280 nm. Portion of the chromatograms is enlarged as shown as inset. All labeled peaks were collected, analyzed by mass spectrometry and summarized in Table 3.

The molecular weight of peak 3 cannot be predicted from the amino acid sequence. However, it corresponds to the predicted molecular weight of the N-terminal heavy chain tryptic peptide with a loss of 18 Da.

3.3. Asn deamidation

MS/MS spectrum of peak 2 is shown in Fig. 5. Y ions from the peptides indicate that deamidation did not occur on the first Asn residue from the C-terminus of the peptide. The only possibility left is deamidation of the Asn residue close to the N-terminus of the peptide. This is further confirmed by comparing the B ions to the predicted B ions from the amino acid sequence. B_3 ion from peak 2 peptide of the stability sample has a 1 Da increase compared to the predicted B_3 ion. MS/MS spectrum of peak 4 is shown in Fig. 6. Y_6 from peak 4 of the stability sample had a 1 Da increase when compared to the predicted Y_6 from the amino acid sequence, which suggests that deamidation occurred on the second Asn residue from the C-terminus of the peptide. Deamidation of Asn usually generates isoAsp and Asp at about 3:1 ratio [9]. Peak 2 has a retention time of 87 min, which is probably the deamidated peptide containing Asp residue because it elutes later than the original Asn peptide, which has a retention time of 85 min [10]. Peak 4 was probably the deamidated

Table 1
Fragments collected from SEC

Residues	Calculated mass (Da)	Observed mass (Da)	Cleavage site
HC330–450	13524	13524	Asn-Lys
HC338–450	12704	12704	Glu-Lys
HC338–450 (+16 Da)	12720	12720	Glu-Lys
HC342–450	12275	12275	Ser-Lys
HC342–450 (+16 Da)	12790	12291	Ser-Lys
LC1–213	23305	23304	Glu-Cys
LC linked to HC1–225	47315	47312	Asp-Lys
LC linked to HC1–225 (−18 Da)	47297	47298	Asp-Lys
LC linked to HC1–228	47681	47681	His-Thr

Table 2
Fragments collected from C4

Peak	Residues	Calculated mass (Da)	Observed mass (Da)	Cleavage site
1	HC330–450	13524	13523	Asn-Lys
	HC330–450 (+K)	13652	13652	Asn-Lys
	HC338–450	12704	12704	Glu-Lys
	HC338–450 (+16 Da)	12720	12721	Glu-Lys
	HC342–450	12275	12275	Ser-Lys
	HC342–450 (+16 Da)	12291	12291	Ser-Lys
2	HC241–450	25204	25205	Gly-Gly
3	LC1–213	23305	23305	Glu-Cys
4	Intact IgGl	148082	148090	None
5	Intact IgGl	148082	148082	None
	LC linked to HC1–225	47315	47315	Asp-Lys
	LC linked to 1–225 (−18 Da)	47297	47297	Asp-Lys
	LC linked to HC1–228	47681	47681	ffis-Thr
	HC275–450	21480	21480	Asp-Pro
	HC275–450 (+E)	21608	21609	Asp-Pro
	HC275–450 (+Gal)	21642	21643	Asp-Pro
6	Intact IgGl	148082	148082	None
	HC1–222	23603	23603	Lys-Ser
	HC1–223	23690	23691	Ser-Cys
7	LC	23408	23408	None
8	Intact IgGl	148082	148084	None

K, C-terminal lysine residue; Gal, addition of galatose to the oligosaccharides.

Table 3
Fragments collected from C4 after reduction

Peak	Residues	Calculated mass (Da)	Observed mass (Da)	Cleavage site
1	HC330–450	13524	13524	Asn-Lys
	HC3 30–450 (+K)	13652	13652	Asn-Lys
	HC331–450	13396	13396	Lys-Ala
	HC338–450	12704	12704	Glu-Lys
	HC338–450 (+16 Da)	12720	12721	Glu-Lys
	HC342–450	12275	12275	Ser-Lys
	HC342–450 (+16 Da)	12291	12291	Ser-Lys
	HC343–450	12147	12147	Lys-Ala
	HC345–450	11947	11947	Lys-Gly
	HC345–450 (+16 Da)	11963	11964	Lys-Gly
2	HC275–450 (Gal 0)	21481	21481	Asp-Pro
	HC275–450 (Gal 1)	21643	21642	Asp-Pro
3	HC241–450	25204	25204	Gly-Gly
4	LC (2SS +1SH)	23408	23408	None
5	LC		23564	LC related
			23583	LC related
6	LC (5SH)	23412	23411	None
7	HC (11SH)	50645	50644	None
8	HC (4SS+3SH)	50637	50635	None
9	HC1–225	23913	23913	Asp-Lys
	HC1–225 (−18 Da)	23895	23895	Asp-Lys
10	LC (2SS +1SH)	23408	23408	None
11	LC (5SH	23412	23411	None
12	HC (4SS +3SH)	50637	50639	None

K, C-terminal lysine residue; Gal, addition of galatose to the oligosaccharides; xSS, number of disulfide bonds; xSH, number of free cysteines.

form containing IsoAsp residue because it eluted earlier than the original Asn peptide [10].

Earlier eluted peptides (before 10 min as shown in Fig. 4) were analyzed using LCQ$_{DECA}$XP instrument. The isotopic distribution of peptides with molecular weight (MH^+) of 447.2 Da from the stability sample was significantly different from that of the control sample (Fig. 7). There are two predicted tryptic peptides with molecular weights of 447.2 Da. Therefore, to avoid having peptides with the same MW, the samples were digested with Lys-C, which produced only one peptide with a MW (MH^+) of 447.2 Da and an amino acid sequence, VSNK. Peptide VSNK from the stability sample had a much more intense (M + 1) peak than what was observed in the control. This was due to a significant percentage of VSNK peptide with a MW increase of 1 Da, which indicates that Asn residue in this peptide was deamidated.

3.4. Gln deamidation

MS/MS spectrum of peak 1 is shown in Fig. 8. The predicted Y ions were observed up to Y_{11}, which indicates that the first Gln from the C-terminus was not deamidated. Therefore, deamidation must have occurred on the Gln residue on the second Gln of the peptide from the C-terminus. The signals of Y ions higher than Y_{11} were too weak to be reliable. B_3 had an increase of 1 Da when compared to the predicted B_3 which confirms that deamidation occurred on the second Gln residue from the C-terminus of the peptide.

3.5. Pyroglutamate

Peak 3 had a molecular weight of 1606.8 Da, which corresponds to the N-terminal tryptic peptide of the heavy chain with a loss of 18 Da. Loss of 18 Da is probably due to cyclization of the N-terminal Glu residue and formation of a pyroglutamate. Peak 3 was digested with pyroglutamate aminopeptidase and then analyzed using MALDI-TOF mass spectrometer. As shown in Fig. 9, after pyroglutamate aminopeptidase digestion, peptide 1606.8 Da was no longer observed and a new peptide with molecular weight of 1495.8 Da appeared. The difference corresponds to a loss of pyroglutamate of 111 Da.

4. Discussion

Protein instability can be classified as either chemical or physical instability [11]. Chemical instability involves covalent bond modifications, while physical instability does not. Aggregation,

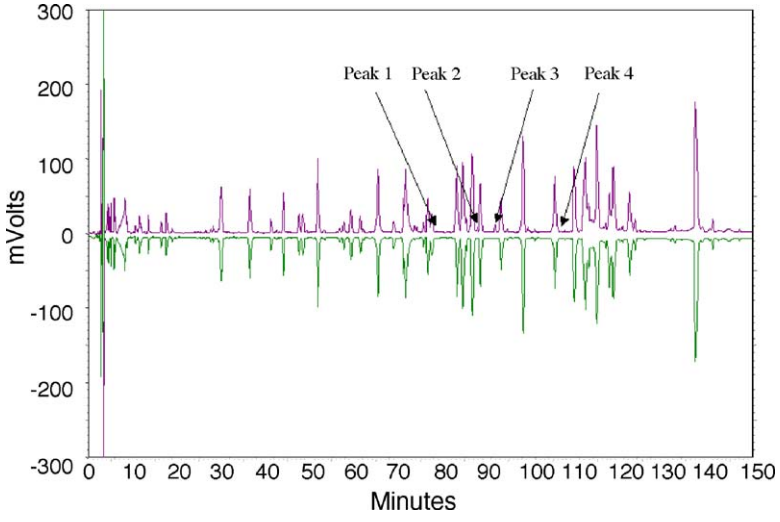

Fig. 4. Mirror image of peptides from accelerated stability sample and control using a 250 mm × 4.6 mm Vydac C18 column and monitored by UV 214 nm. Peaks 1–4 were collected and analyzed by mass spectrometry.

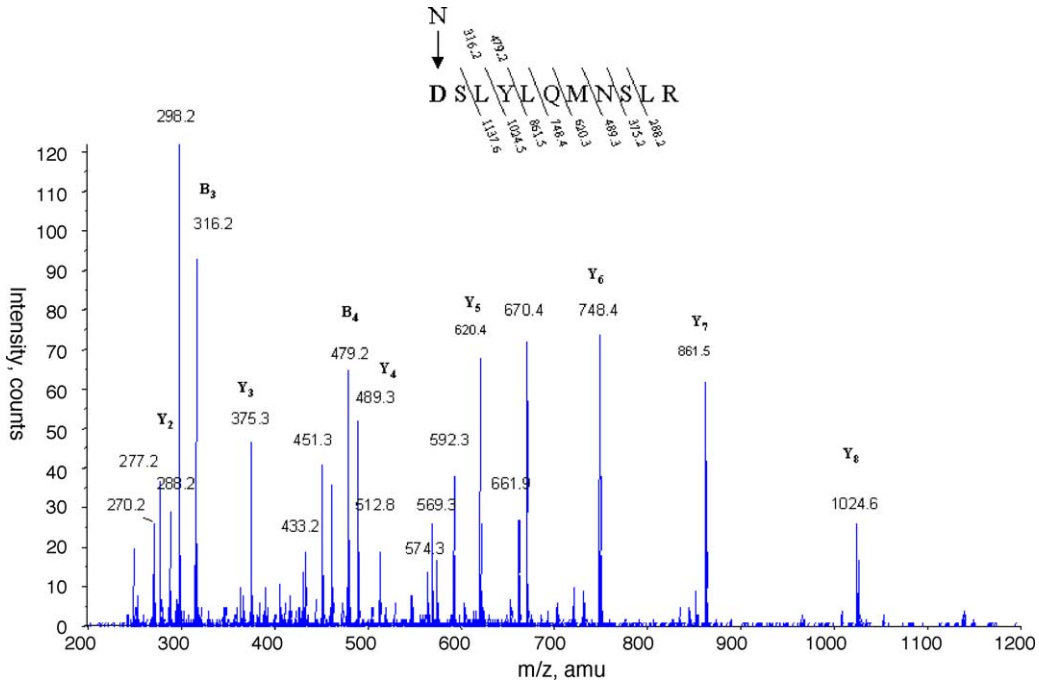

Fig. 5. MS/MS spectrum of peak 2 from Fig. 4. The amino acid sequences and predicted Y ions and B ions are shown as inset. The observed mass of Y ions and B ions are shown in the spectrum and labeled accordingly.

which is considered a physical instability, is not the major degradation pathway for this fully human monoclonal IgG_1 antibody even after storage at 40 °C for 6 months. However, significant chemical degradation was found in the stability samples including peptide bond cleavage, Asn deamidation, Gln deamidation and N-terminal Glu cyclization to form pyroglutamate.

The most flexible region of IgG molecules is in the hinge region [12]. Peptide bond cleavage around the hinge region has been reported for OKT3 [3], a murine IgG2a antibody. The cleavage site was located between hinge amino acids Cys and Pro. Two major cleavage sites between hinge amino acids Asp-Lys and His-Thr were also reported for four humanized IgG_1

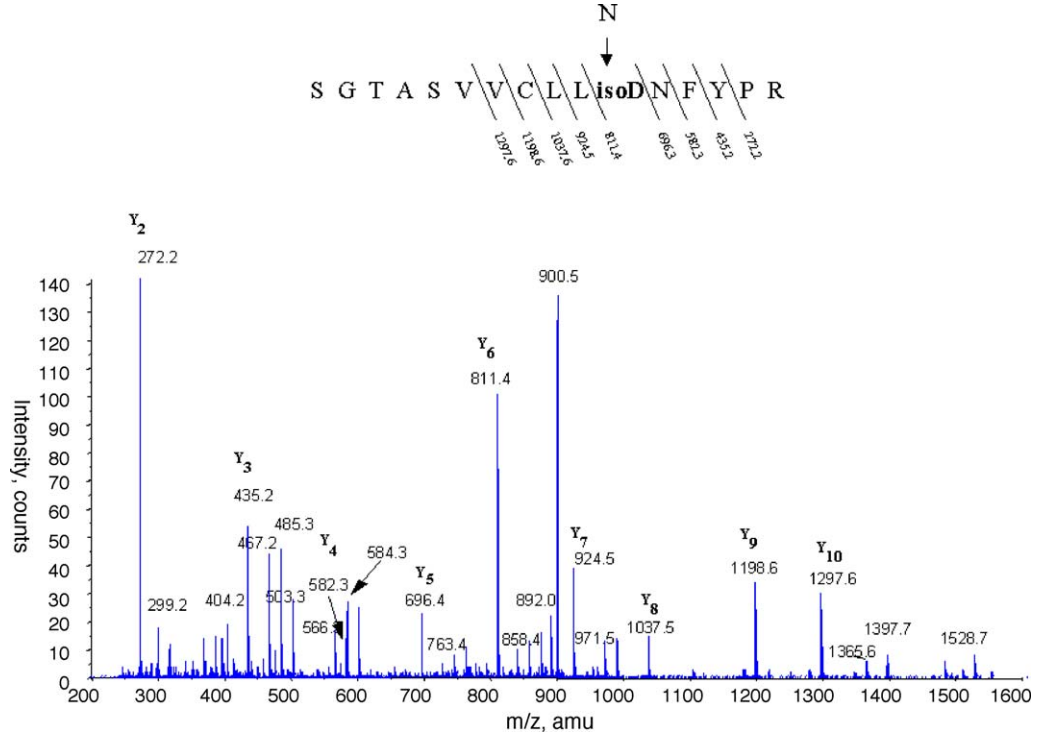

Fig. 6. MS/MS spectrum of peak 4 from Fig. 4. The amino acid sequences and predicted Y ions and B ions are shown as inset. The observed mass of Y ions and B ions are shown in the spectra and labeled accordingly.

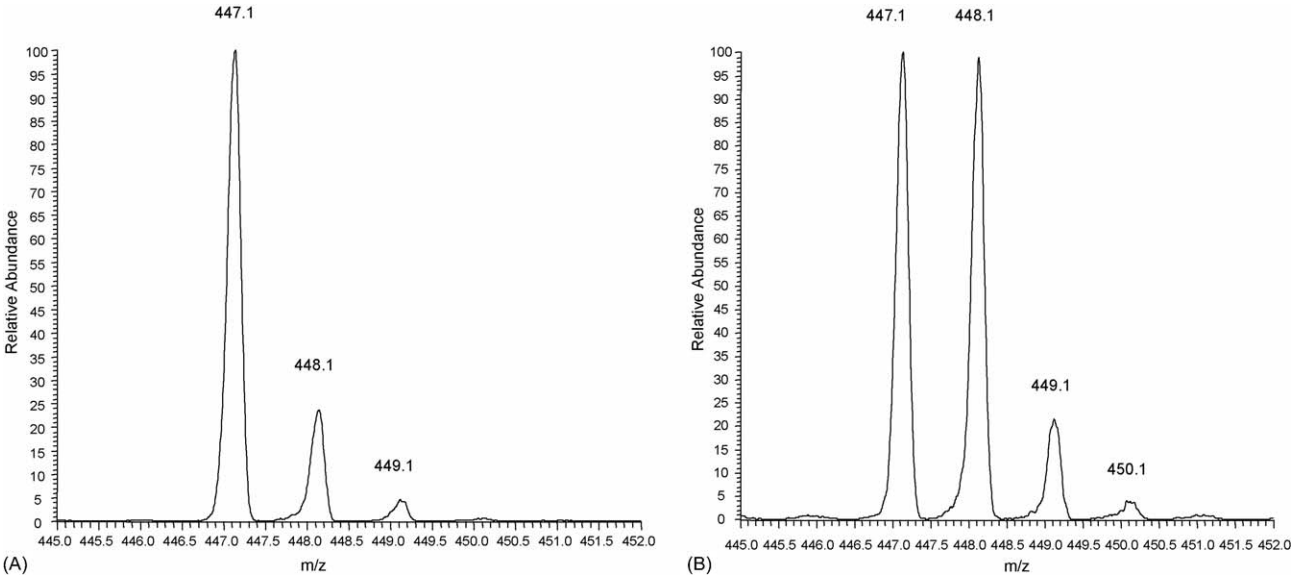

Fig. 7. Zoom scans of peptide VSNK from the accelerated stability sample and control obtained after Lys-C digestion and monitored using LCQ$_{DECA}$XP mass spectrometer. Zoom scan from (A) control sample and (B) the accelerated stability sample.

monoclonal antibodies [6]. In agreement with previous studies, peptide bond cleavage between hinge amino acids Asp-Lys and His-Thr were also found in the stability samples of our study. Cleavage in the Fc region was also observed. Although several cleavage sites were normally identified in close proximity, it is possible that the initial cleavage resulted in a larger fragment and the fragment further degraded after disassociation from the molecule. For example, cleavage between heavy chain amino acids 337–338 and 341–342 most likely occurred after the initial cleavage of heavy chain amino acids 329–330. Applying the same rationale to all the fragments, it is clear that cleavage of peptide bonds occurred in three major regions. The first cleavage region is located in the hinge region. The second region is around the CH_2 and CH_3 interface. The IgG_1 molecules are well folded especially CH_2 and CH_3 domains [12]. But, the interface of CH_2 and CH_3 domain is less stable as evidenced by the relative accessibility to proteases after low pH incubation [13]. The third region most likely originated with the cleavage of peptide bond between amino acids Asp274 and Pro275. Asp-Pro is a well-known susceptible site for peptide bond cleavage [11].

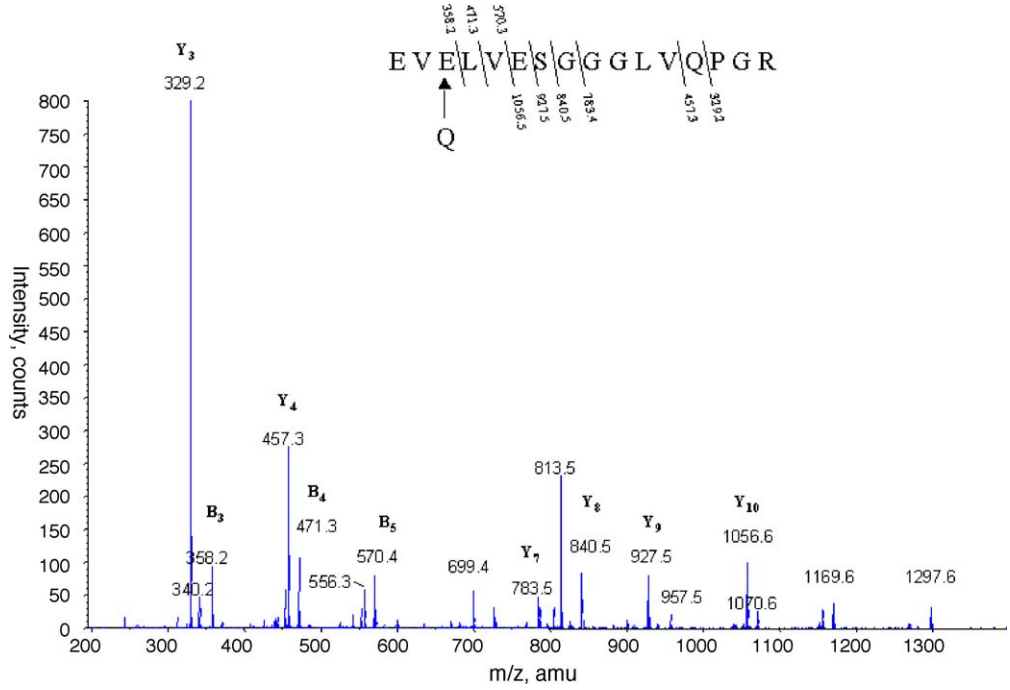

Fig. 8. MS/MS spectrum of peak 1 from Fig. 4. The amino acid sequences and predicted Y ions and B ions are shown as inset. The observed mass of Y ions and B ions are shown in the spectra and labeled accordingly.

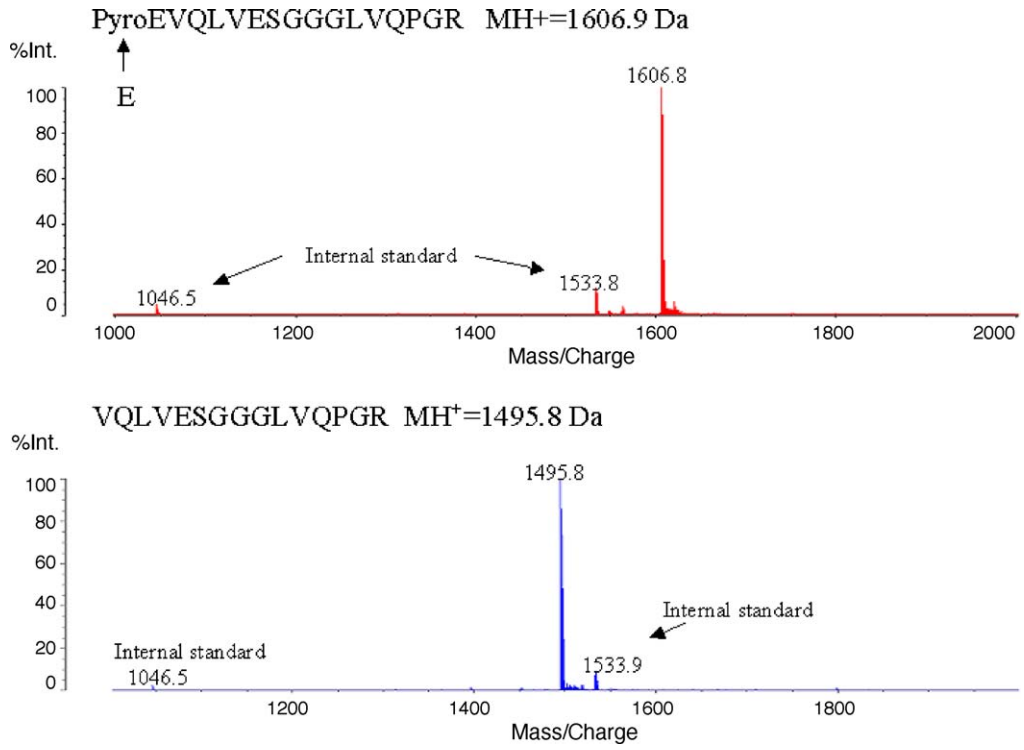

Fig. 9. MALDI-TOF mass spectra of peak 3 from Fig. 4. Top: material from peak 3. Shown as inset are the amino acid sequence and its calculated molecular weight. Bottom: peak 3 after pyroglutamate aminopeptidase treatment. Shown as inset is the amino acid sequence and its molecular weight.

Several fragments with a molecular weight increase of 16 Da were observed. The 16 Da increase is probably due to oxidation of methionine or other residues [2,3]. Interestingly, we also observed a modified fragment of HC1-225 with a molecular weight of 18 Da less than what was predicted from the sequence. A similar modification was reported by Cordoba et al. [6]. The loss of 18 Da could be due to the formation of an anhydride intermediate [14,15] or formation of an anhydride of the C-terminal Asp after peptide bond cleavage [6]. Modifications such as formation of pyroglutamate, or intramolecular peptide bonds are also possible. Peak 5 contains two fragments with molecular weights of 23,564 and 23,583 Da, respectively, which are approximately 155 and 174 Da higher than the observed light chain molecular weight. Trypsin digestion of peak 5 showed that the majority of peaks with intense signals were from light chain. Therefore, these fragments are probably modified light chain. It was also interesting to note that different molecular weights of intact light chains and heavy chains in the stability sample were observed. It was shown that only interchain disulfide bonds can be reduced when reduction was carried out under native conditions [16]. Thus, a higher molecular weight may reflect partial reduction of intrachain disulfide bonds of the stability sample or conformational changes that led to different positioning of some disulfide bonds that become readily reduced.

Deamidation is a major non-enzymatic protein degradation pathway [17]. Deamidation of Asn residues has been reported for several monoclonal antibodies [2,7,8,18–20]. Therefore, not surprisingly, three Asn deamidation sites were observed in the stability sample in this study. Deamidation has been reported to occur mostly on an Asn residue that is followed by a Gly residue at peptide level [9,21] and protein level [17]. There are two such sites on the Fc region on each of the heavy chains of this antibody. However, neither one was found to deamidate to a detectable level. Asn followed by Ser was also reported to be susceptible to deamidation [17]. In this study, one Asn followed by a Ser was found to deamidate. Three-dimensional structure also plays a critical role in affecting Asn deamidation rate [22–27]. Thus, the two predicted sites most susceptible to deamidation are likely protected in this antibody by the native structures. Deamidation of Gln can follow similar mechanisms as Asn deamidation [9]. At low pH, deamidation of Gln could be a result of direct hydrolysis as reported for glucagons [15]. Non-enzymatic deamidation of Gln has a much slower rate than the deamidation rate of Asn residues [28]. Among a total of 62 Gln residues in the antibody in this study, only one Gln was deamidated to a detectable amount after incubation at 40 °C for 6 months. This Gln is the third residue from the N-termini of the heavy chains, which probably has a larger surface accessibility than the other Gln residues. Deamidation of this Gln residue could also occur on antibody fragments, which would have less structural restrictions and more flexibility and exposure. Deamidation of Gln has also been reported as a result of transglutaminase or protein with transglutaminase activity such as the cytotoxic necrotizing factor from *Escherichia coli* [29,30], which is unlikely to be the cause of the single low level Gln deamidation discovered in this study.

Formation of pyroglutamate has been reported for several monoclonal antibodies [31–33], and all were formed from N-

terminal Gln, not Glu. Formation of pyroglutamate from Glu is less common than from Gln. However, there are reports that pyroglutamate can be formed from Glu including β-lipotropin and joining peptide [34], amyloid β protein [35], and in neurons [36]. In three cases, there is some debate on whether cyclization of Glu is due to an enzymatic reaction. However, non-enzymatic formation of pyroglutamate from Glu has been reported at the free amino acid level when Glu was incubated at high temperature and low pH [37]. Discovery of low levels of spontaneous formation of pyroglutamate in this study adds an example to non-enzymatic pyroglutamate formation.

In summary, the stability of a recombinant fully human monoclonal antibody was characterized after storage at 40 °C for 6 months. Peptide cleavage was observed at several different sites between different pairs of amino acids. Deamidation was mainly detected at three Asn residues. One of them was in a short peptide, which could be easily overlooked. This observation validated the value of applying orthogonal analytical techniques in protein characterization. Deamidation of a Gln residue was also observed. Interestingly, partial conversion of the N-terminal Glu of heavy chain to pyroglutamate was also present in the stability samples.

Acknowledgements

The authors would like to thank Brian G. Turner and Peter Moesta for their support and careful review of the manuscript.

References

[1] W. Jiskoot, E.C. Beuvery, A.A. de Koning, J.N. Herron, D.J. Crommelin, Pharm. Res. 7 (1990) 1234.
[2] D.J. Kroon, A. Baldwin-Ferro, P. Lalan, Pharm. Res. 9 (1992) 1386.
[3] P.E. Rao, D.J. Kroon, Pharm. Biotechnol. 5 (1993) 135.
[4] M. Paborji, N.L. Pochopin, W.P. Coppola, J.B. Bogardus, Pharm. Res. 11 (1994) 764.
[5] A.J. Alexander, D.E. Hughes, Anal. Chem. 67 (1995) 3626.
[6] A.J. Cordoba, B.J. Shyong, D. Breen, R.J. Harris, J. Chromatogr. B Anal. Technol. Biomed. Life Sci. 818 (2005) 115.
[7] P.K. Tsai, M.W. Bruner, J.I. Irwin, C.C. Ip, C.N. Oliver, R.W. Nelson, D.B. Volkin, C.R. Middaugh, Pharm. Res. 10 (1993) 1580.
[8] M. Perkins, R. Theiler, S. Lunte, M. Jeschke, Pharm. Res. 17 (2000) 1110.
[9] T. Geiger, S. Clarke, J. Biol. Chem. 262 (1987) 785.
[10] D.W. Aswad, A.W. Guzzetta, in: D.W. Aswad (Ed.), Deamidation and Isoasparate Formation in Peptides and Proteins, CRC Press, Boca Raton, FL, 1995, p. 7.
[11] M.C. Manning, K. Patel, R.T. Borchardt, Pharm. Res. 6 (1989) 903.
[12] L.J. Harris, E. Skaletsky, A. McPherson, J. Mol. Biol. 275 (1998) 861.
[13] J.R. Ellerson, D. Yasmeen, R.H. Painter, K.J. Dorrington, J. Immunol. 116 (1976) 510.
[14] T.V. Brennan, S. Clarke, Int. J. Pept. Protein Res. 45 (1995) 547.
[15] A.B. Joshi, M. Sawai, W.R. Kearney, L.E. Kirsch, J. Pharm. Sci. 94 (2005) 1912.
[16] D.W. Sears, J. Mohrer, S. Beychok, Biochemistry 16 (1977) 2031.
[17] H.T. Wright, Crit. Rev. Biochem. Mol. Biol. 26 (1991) 1.
[18] W. Zhang, M.J. Czupryn, J. Pharm. Biomed. Anal. 30 (2003) 1479.
[19] R.J. Harris, B. Kabakoff, F.D. Macchi, F.J. Shen, M. Kwong, J.D. Andya, S.J. Shire, N. Bjork, K. Totpal, A.B. Chen, J. Chromatogr. B Biomed. Sci. Appl. 752 (2001) 233.
[20] L. Wang, G. Amphlett, J.M. Lambert, W. Blattler, W. Zhang, Pharm. Res. 22 (2005) 1338.
[21] N.E. Robinson, A.B. Robinson, Proc. Natl. Acad. Sci. USA 98 (2001) 944.
[22] N.E. Robinson, A.B. Robinson, Proc. Natl. Acad. Sci. USA 98 (2001) 12409.
[23] T.V. Brennan, J.W. Anderson, Z. Jia, E.B. Waygood, S. Clarke, J. Biol. Chem. 269 (1994) 24586.
[24] S. Clarke, Int. J. Pept. Protein Res. 30 (1987) 808.
[25] T.V. Brennan, S. Clarke, Protein Sci. 2 (1993) 331.
[26] D.W. Aswad, M.V. Paranandi, B.T. Schurter, J. Pharm. Biomed. Anal. 21 (2000) 1129.
[27] B.A. Johnson, N.E. Freitag, D.W. Aswad, J. Biol. Chem. 260 (1985) 10913.
[28] A.B. Robinson, J.W. Scotchler, J.H. McKerrow, J. Am. Chem. Soc. 95 (1973) 8156.
[29] G. Flatau, E. Lemichez, M. Gauthier, P. Chardin, S. Paris, C. Fiorentini, P. Boquet, Nature 387 (1997) 729.
[30] G. Schmidt, J. Selzer, M. Lerm, K. Aktories, J. Biol. Chem. 273 (1998) 13669.
[31] D.A. Lewis, A.W. Guzzetta, W.S. Hancock, M. Costello, Anal. Chem. 66 (1994) 585.
[32] W.E. Werner, S. Wu, M. Mulkerrin, Anal. Biochem. 342 (2005) 120.
[33] L. Wang, G. Amphlett, W.A. Blattler, J.M. Lambert, W. Zhang, Protein Sci. 14 (2005) 2436.
[34] S.L. Knock, G.T. Nagle, C.Y. Lin, D.J. McAdoo, A. Kurosky, Peptides 10 (1989) 859.
[35] H. Mori, K. Takio, M. Ogawara, D.J. Selkoe, J. Biol. Chem. 267 (1992) 17082.
[36] R.W. Garden, T.P. Moroz, J.M. Gleeson, P.D. Floyd, L. Li, S.S. Rubakhin, J.V. Sweedler, J. Neurochem. 72 (1999) 676.
[37] C.B. Park, S.B. Lee, D.D. Ryu, Appl. Environ. Microbiol. 67 (2001) 3650.